

Sự trao đổi và hấp phụ các cation kim loại trên bề mặt kaolinite: Nghiên cứu thuyết phiếm hàm mật độ

TÓM TẮT

Trong nghiên cứu này các quá trình trao đổi và hấp phụ các cation kim loại được khảo sát sử dụng các tính toán lý thuyết phiếm hàm mật độ. Các kết quả thu được chỉ ra rằng, các sự trao đổi cation hàm như không thuận lợi, trong đó các vị trí Al^{3+} dễ thay thế hơn Si^{4+} . Các cation kim loại được hấp phụ mạnh mẽ trên kaolinite ở cả hai mặt H-slab và O-slab. Kết quả tính tại phiếm hàm PBE, khả năng hấp phụ các cation kim loại giảm theo thứ tự $\text{Li}^+ > \text{K}^+ > \text{Na}^+ > \text{Ca}^{2+} > \text{Al}^{3+} > \text{Fe}^{3+} > \text{Cr}^{3+} > \text{Mg}^{2+}$. Đáng chú ý, sự xâm nhập vào cấu trúc tinh thể của kaolinite được phát hiện đối với Li^+ và Mg^{2+} ở mặt H-slab cùng với sự hình thành các liên kết mới Li-O và Mg-O. Trong khi đó, sự xen vào giữa các lớp kaolinite bởi các cation Ca^{2+} được phát hiện với sự hình thành các liên kết Ca-O với cả hai mặt H-slab và O-slab. Các phân tích mật độ trạng thái và phân bố electron định vị chứng tỏ sự hình thành các liên kết hóa học mới M-O trong quá trình hấp phụ. Hơn nữa, K^+ được đề xuất như là sự thêm vào tiềm năng đối với các bề mặt kaolinite trong sự hấp phụ các hợp chất hữu cơ trong các môi trường.

Từ khóa: *Sự trao đổi, hấp phụ, cation kim loại, DFT.*

Metal cation exchange and adsorption onto kaolinite surfaces: A DFT study

ABSTRACT

In this study, metal cations' exchange and adsorption processes onto kaolinite surfaces are investigated using density functional theory calculations. Obtained results indicate that the exchanges of cations are mostly unfavorable, and the Al sites are conveniently replaced compared to Si sites. The metal cations are adsorbed strongly onto kaolinite surfaces at both O-slab and H-slab. The adsorption ability of metal cations decreases in the order of $\text{Li}^+ > \text{K}^+ > \text{Na}^+ > \text{Ca}^{2+} > \text{Al}^{3+} > \text{Fe}^{3+} > \text{Cr}^{3+} > \text{Mg}^{2+}$ at the PBE functional. Remarkably, the insertions of Li^+ and Mg^{2+} into the lattice structure of kaolinite are found at H-slab following the Li-O, Mg-O new bonds formation. While the intercalation into kaolinite by Ca^{2+} is observed in forming Ca-O bonds with both H-slab and O-slab. The analyses of the density of states and electron localization function clarify the appearance of M-O chemical bonding upon the adsorption process. Further, K^+ is suggested as a promising addition to kaolinite surfaces for the adsorption of organic compounds in environments.

Keywords: Exchange, Adsorption, Metal cations, DFT.

1. INTRODUCTION

Kaolinite is one of two-layer alumosilicate minerals, with two types of surface structure: hydrogen-rich surface (H-slab) and oxygen-rich surface (O-slab). The H-slab surface with high positive charge density is favorable for interaction with organic compounds containing functional groups such as -OH, - COOH.¹⁻³ In addition, the adsorptions of benzene, n-hexane, pyridine, and 2-propanol on H-slab are more substantial than those on O-slab.⁴ In contrast, the O-slab containing a sizeable negative charge density is considered an efficient surface for the adhesion of metal cations or other cations. As a result, kaolinite is one of the potential materials in the adsorption and removal of heavy metals from aquatic environments.⁵ Besides, theoretical approaches using density functional theory (DFT) provide insight into the adsorption process of metal cations on material surfaces.

It is noticeable that the exchange of cations in the material structure leads to considerable changes in electronic and surface properties, increasing materials' applicability, especially in energy and environment fields.⁶ In the present work, we use DFT calculations to investigate the

exchange of cations in the lattice structure of kaolinite with different metal cations, thereby gaining insight into the structural and electronic properties. Besides, the adsorption of various metal cations on kaolinite surfaces is observed to evaluate the suitable consistency. Furthermore, theoretical results are expected to suggest promising metal cations adding to the kaolinite surfaces for the adsorption and removal of organic pollutants in environments.

2. COMPUTATIONAL METHOD

The geometric structures of the kaolinite surfaces and adsorption configurations are optimized by VASP.⁷ Kaolinite is one of the common clay minerals, including a series of uncharged layers connected by a network of hydrogen bonds between H-slab and O-slab, as shown in Figure 1. In this work, the $1 \times 1 \times 1$ (for one layer in exchange) and $2 \times 1 \times 1$ (for two layers in adsorption) cell models are designed with dimensions size: $a = 5.15 \text{ \AA}$; $b = 8.93 \text{ \AA}$; $c = 7.38 \text{ \AA}$, and $a = 10.30 \text{ \AA}$; $b = 8.93 \text{ \AA}$; $c = 28.51 \text{ \AA}$, respectively. The vacuum space in the two-layers model is about 15 \AA , large enough to ignore boundary interactions between two slabs. Plane-wave cutoff energy is set up at 500 eV upon optimization.

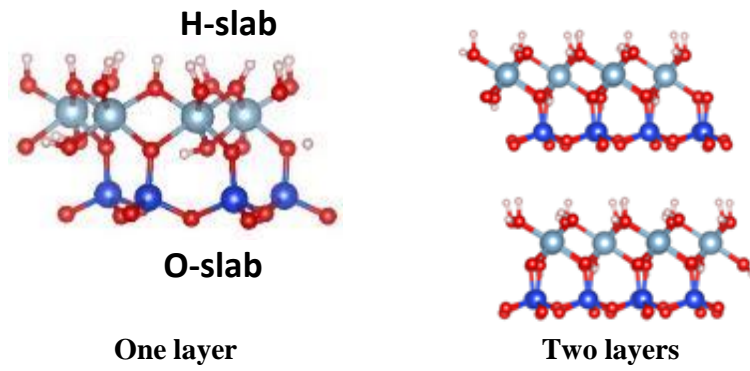


Figure 1. The cell models of kaolinite in this work

In addition, the Perdew-Burke-Ernzerhof (PBE) function with a generalized gradient approximation (GGA) for the exchange-correlation component is used in all calculations.⁸ Adsorption energy (E_{ads}) is computed by using the following expressions: $E_{\text{ads}} = E_{\text{comp}} - E_{\text{kaoli}} - E_M$, where E_{comp} , E_{kaoli} , and E_M are the energy values of complexes, kaolinite surfaces, and metal cations, respectively. The exchange energy (E_{exh}) of metal cations into the lattice structure of kaolinite is determined as follows: $E_{\text{exh}} = E_{\text{kaoli}-M} + E_{\text{Al/Si}} - E_M - E_{\text{kaoli}}$ in which $E_{\text{kaoli}-M}$ and $E_{\text{Al/Si}}$ correspond to the energy values of the new structure of cation exchange and $\text{Al}^{3+}/\text{Si}^{4+}$. Moreover, to understand the formation of stable structures, the density of states (DOS) and electronic localization function (ELF) analyses are carried out at the same level of theory.

3. RESULTS AND DISCUSSION

3.1. Optimized structures

The stable configurations of exchange and adsorption of metal cations (M), including Li^+ , Na^+ , K^+ , Mg^{2+} , Ca^{2+} , Al^{3+} , Cr^{3+} , and Fe^{3+} based on

DFT calculations at PBE functional, are presented in Figure 2. Accordingly, the cation exchange occurs at Al^{3+} or Si^{4+} sites of kaolinite lattice structure. Some Al-O or Si-O bonds are broken and replaced by new M-O bonds upon optimization. The bond lengths of Al/Si-O in kaolinite are ca. 1.85-2.00 Å (Al) and 1.61-1.64 Å (Si), consistent with experiment values in previous studies.⁹ For derivatives in exchange, the M-O bond lengths for replacement of Al^{3+} (denoted by M1) and Si^{4+} (denoted by M2) sites are 1.97-2.24 Å (Li1), 1.80-1.89 Å (Li2), 2.13-2.37 Å (Na1), 2.08-2.17 Å (Na2), 2.35-2.89 Å (K1), 2.30-3.15 Å (K2), 1.99-2.07 Å (Mg1), 1.86-1.92 Å (Mg2), 2.18-2.30 Å (Ca1), 2.11-2.73 Å (Ca2), 1.73-1.75 Å (Al2), 1.84-1.99 Å (Si1), 1.91-2.03 Å (Cr1), 1.72-1.80 Å (Cr2), 1.88-2.01 Å (Fe1), 1.73-1.81 Å (Fe2). As a result, the M-O distances are larger at M2 than at M1 structures following the cation exchange. Moreover, the charge densities surrounding Al/Si sites in kaolinite change in replacing metal cations. Hence, the cation substitutions lead to considerable changes in M-O bond length and charge density on M, which could cause a decrease in structure strength compared to initial kaolinite.

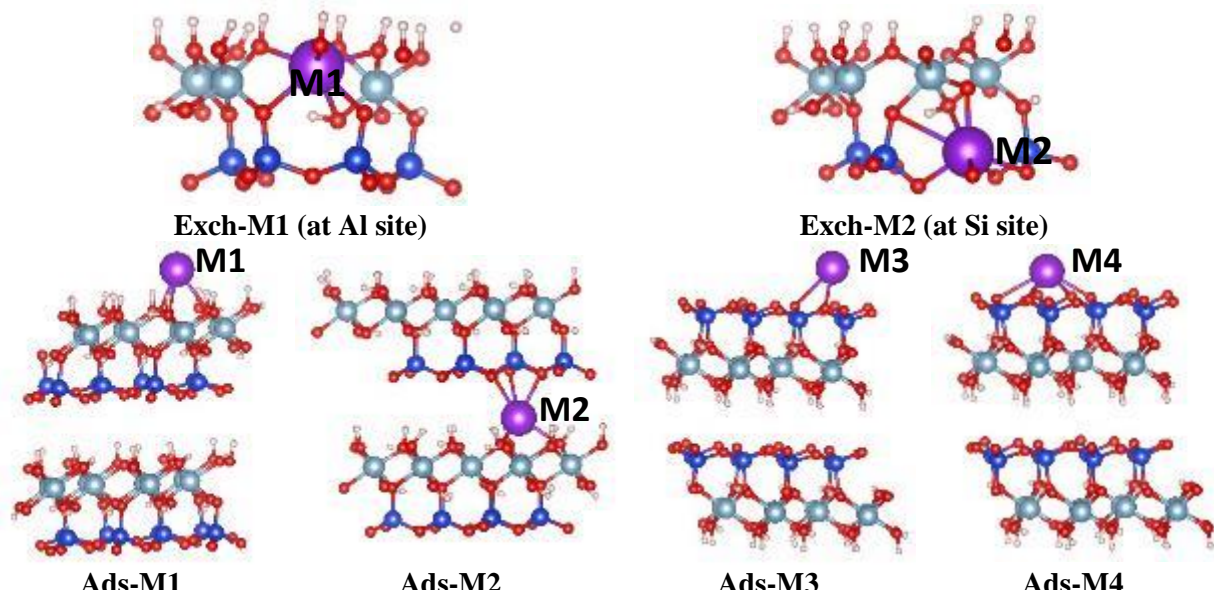


Figure 2. The optimized structures of cations exchange and adsorption on kaolinite surfaces

In addition, the adsorption of metal cations onto kaolinite is observed at the H-slab, O-slab, and between two of these slabs, as displayed in Figure 2. Metal cations attach on H-slab at the O sites to form M-O interactions (**Ads-M1**), while the adhesion of metal cations on O-slab is preferred at the tetragonal cage (**Ads-M3**) and hexagonal cage (**Ads-M4**). The attachment of cations into the interlayer of H-slab and O-slab is considered in the present work. Here, the configurations are stabilized by M-O new bonds (**Ads-M2**). The interaction distances in adsorption configurations (**Ads-M1**, **Ads-M2**, **Ads-M3**, **Ads-M4**) are mostly larger than M-O bond lengths in cation exchange. In particular, the M-O distances are ca. 2.66-2.69 (Li1), 2.04-2.29 (Li2), 1.90-2.57 (Li3), 2.08-2.50 (Li4), 2.45-2.50 (Na1), 2.27-2.90 (Na2), 2.35-2.66 (Na3), 2.39-2.95 (Na4), 2.80-

2.82 (K1), 2.49-3.02 (K2), 2.65-3.06 (K3), 2.75-3.14 (K4), 2.22 (Mg1), 2.05-2.14 (Mg2), 2.92 (Mg3), 3.25 (Mg4), 2.42 (Ca1), 2.32-2.73 (Ca2), 2.40 (Ca3), 2.47-2.50 (Ca4), 2.01 (Al1), 2.14-3.08 (Al2), 2.16 (Al3), 2.31-2.94 (Al4), 2.50-2.65 (Cr1), 2.13-3.02 (Cr2), 2.27 (Cr3), 2.28 (Cr4), 2.38-2.69 (Fe1), 1.97-3.56 (Fe2), 2.23 (Fe3), 2.45-2.92 (Fe4) upon adsorptions. Noticeably, the Li^+ and Mg^{2+} cations tend to insert into the lattice structure of kaolinite and form Li-O and Mg-O new bonds along with Al-O bonds at H-slab.

3.2. Exchange and adsorption energies

The characteristic parameters such as the exchange energy (E_{exh}) and adsorption energy (E_{ads}) calculated and gathered in Table 1 aim to evaluate metal cations' exchange and adsorption ability onto kaolinite surfaces.

Table 1. The energy of cation exchange (E_{exh}) and adsorption (E_{ads}) on kaolinite (in kcal.mol^{-1})

	M	Li^+	Na^+	K^+	Mg^{2+}	Ca^{2+}	Al^{3+}	Cr^{3+}	Fe^{3+}
E_{exh}	Exch-M1	214.7	250.0	282.5	126.1	123.2	--	57.7	96.6
	Exch-M2	284.5	326.5	357.6	210.9	210.6	70.9	92.3	132.8
E_{ads}	Ads-M1	-12.9	-12.1	-12.7	-5.5	-11.8	-22.6	-6.7	-11.7
	Ads-M2	-61.9	-25.9	-14.6	-7.0	-24.3	-12.0	-6.7	-10.5
	Ads-M3	-26.8	-21.4	-25.3	-0.7	-14.2	-18.1	-7.9	-8.1
	Ads-M4	-42.1	-29.8	-33.5	-0.8	-21.6	-17.4	-8.7	-7.1

Calculated results show that the exchange energy of metal cations is highly positive, in the range of $57.7\text{-}357.6\text{ kcal.mol}^{-1}$, indicating these processes are endothermic and thermodynamically unfavorable. Al^{3+} , Cr^{3+} , and Fe^{3+} substitutions by metal cations are more convenient than other cations with small positive E_{exh} values. The cation exchanges are focused at Al^{3+} and Si^{4+} sites, in which the derivatives are more favorable at the Al^{3+} than at Si^{4+} , especially the Cr^{3+} (E_{exh} ca. 57.7 kcal/mol) structure. With the Si^{4+} substitutions, the Al^{3+} (E_{exh} ca. 70.9 kcal/mol) structure is formed more conveniently than metal cations. Here, it can be understood that the changes in charge density and radius of the metal cations in kaolinite yield changes in new geometrical structures. The substituted metal cations mostly have a smaller charge and a much different radius than the substituted $\text{Al}^{3+}/\text{Si}^{4+}$ in kaolinite, leading to less stable systems.

For the adsorption of metal cations onto H-slab and O-slab surfaces, the adsorption energy ranges from -7.0 to $-61.9\text{ kcal.mol}^{-1}$. The obtained configurations are thus relatively stable. The metal cations are adsorbed strongly to different regions onto kaolinite surfaces. Specifically, Li^+ cations tend to insert into the kaolinite in the octahedral cage and form Li-O new bonds in the **Ads-Li2** (E_{ads}

ca. $-61.9\text{ kcal.mol}^{-1}$), the most stable structure in investigated systems. The **Ads-Li4** is a pretty tough configuration with an adsorption energy value of $-42.1\text{ kcal.mol}^{-1}$, which has Li-O bonds formed at the octahedral cage of the O-slab. It is due to the radius of Li^+ being relatively small, the smallest one among the metal cations, so it is conveniently located at cages of H-slab and O-slab and inserted into the lattice structure of kaolinite. Besides, Na^+ , K^+ , and Cr^{3+} cations interact considerably with O sites on the O-slab of kaolinite upon **Ads-Na4**, **Ads-K4**, and **Ads-Cr4** formation with corresponding adsorption energies of -29.8 , -33.5 , and $-8.7\text{ kcal.mol}^{-1}$. These structures are much more stable than **Ads-Na1**, **Ads-K1**, and **Ads-Cr1** (adsorption occurred on the H-slab).

On the other hand, the Al^{3+} and Fe^{3+} cations are located at the H-slab to form M-O interactions at the top of the tetrahedral cage in **Ads-Al1** (E_{ads} of $-22.6\text{ kcal.mol}^{-1}$) and **Ads-Fe1** (E_{ads} of $-11.7\text{ kcal.mol}^{-1}$) configurations. These structures are about $4\text{-}5\text{ kcal.mol}^{-1}$ more stable than **Ads-Al4** and **Ads-Fe4** with adsorption at the O-slab. With the remaining metal cations (Mg^{2+} , Ca^{2+}), the most stable configurations are **Ads-Mg2** and **Ads-Ca2** with the intercalation of ions between the H-slab and O-slab. Noticeably, Mg^{2+} inserts into the H-slab and forms Mg-O bonds similar to Li^+ . However, the **Ads-Mg2** (E_{ads} of $-7.0\text{ kcal.mol}^{-1}$) is

much less stable than **Ads-Li2**. Meanwhile, Ca^{2+} forms Ca-O regular forces with both H-slab and O-slab. The **Ads-Ca2** is thus relatively stable in this case, with an adsorption energy of $-24.3 \text{ kcal.mol}^{-1}$. Furthermore, among the common metal cations in aqueous environments (Na^+ , K^+ , Mg^{2+} , and Ca^{2+}), K^+ has the best adsorption ability on kaolinite surfaces. Hence, K^+ is expected to be a good candidate to support kaolinite surfaces for the

adsorption of organic compounds.

3.3. DOS and ELF analyses

To better understand the formation of structures following the cation exchange and adsorption, the density of states (DOS) and electron localization function (ELF) analyses at the PBE function are examined and illustrated in Figures 3 and 4.

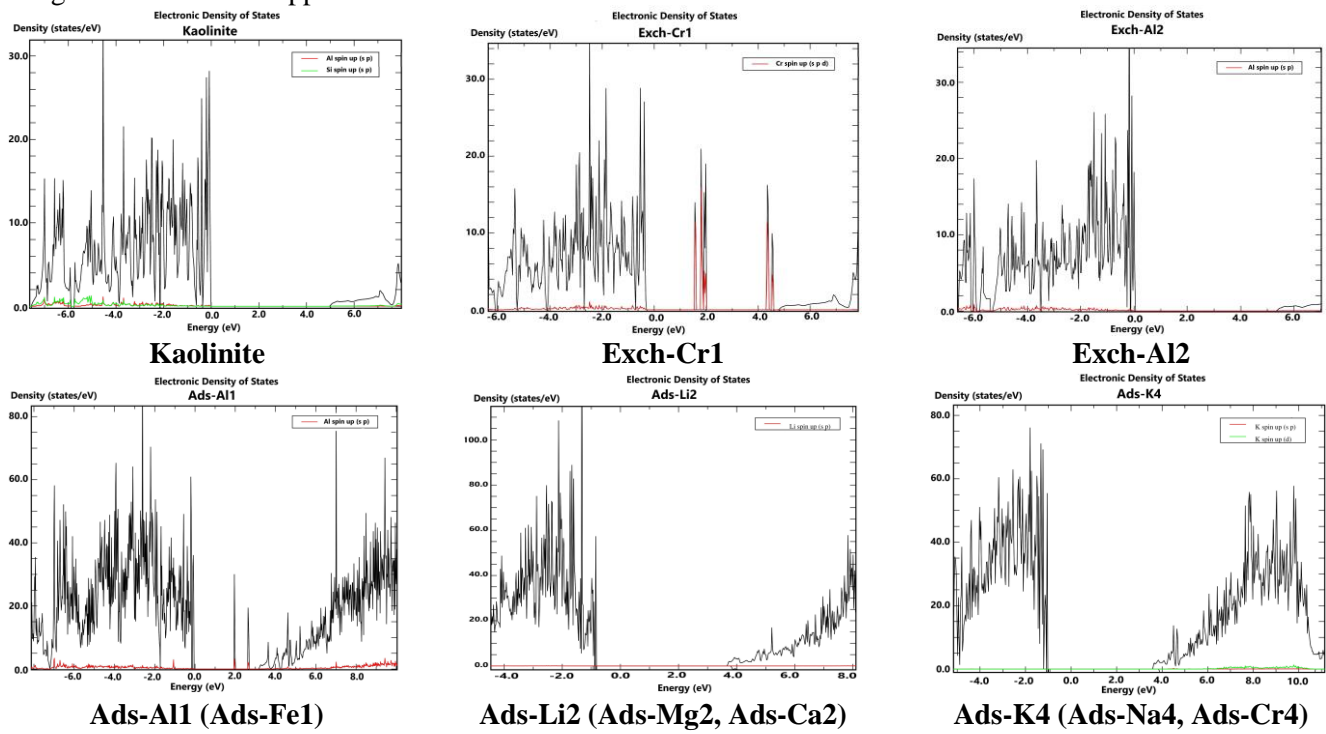


Figure 3. The pDOS of the stable configurations for metal cations exchange and adsorption

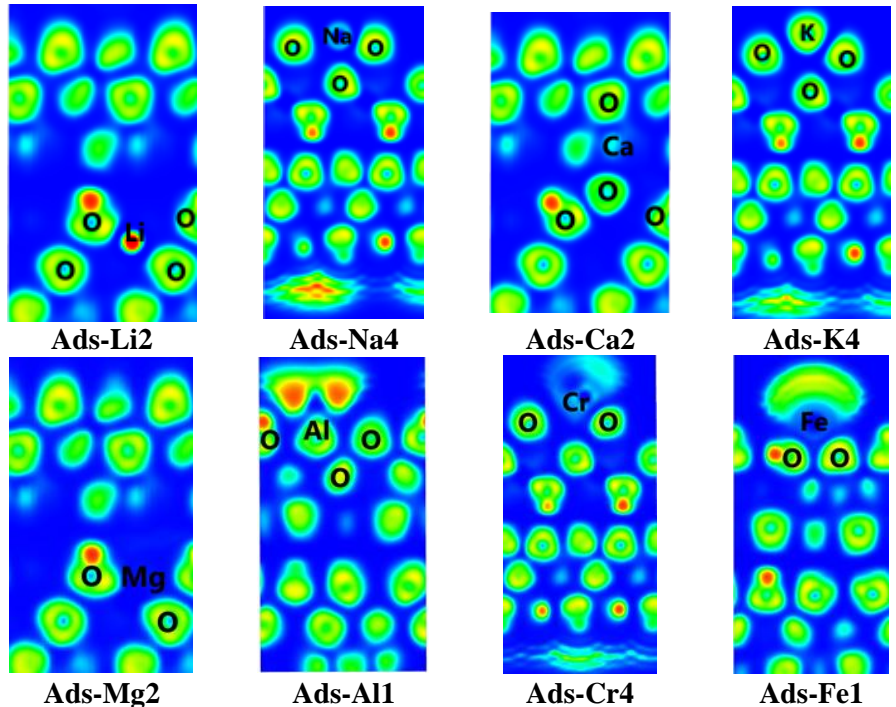


Figure 4. The ELF maps of the adsorption configurations

As shown in Fig.3, there are slight decreases in the density of states (DOS) in the valence band (VB) and conduction band (CB). These two shifts are approximate, so the gap energy (E_g) in obtained structures has little change compared to the initial kaolinite. It is noted that, in the exchange of Al^{3+} , Cr^{3+} , and Fe^{3+} , the hybridizations of the 3p (Al) and 3d (Cr, Fe) orbitals and the 2s and 2p orbitals of O (in kaolinite) lead to form new states as narrow lines between VB and CB. The E -gap of these structures is thus significantly reduced. It can be seen that the cation exchange and adsorption of Al^{3+} , Cr^{3+} and Fe^{3+} would yield better light absorption and increase the photocatalytic activity of the materials compared to the original kaolinite.

Results of ELF analysis indicate that the interactions are formed between M metals and O at the H-slab and O-slab with highly localized electron density, regarded as the chemical bonds.¹⁰ The electron density sharing between M-O bonds is more favorable at the O-slab surface than at the H-slab. Significantly, the electron density localized at the M-O bonds for the structures is considerably high and decreases from **Ads-Li2**, **Ads-K4**, and **Ads-Na4**, going to **Ads-Ca2**, **Ads-Al1**, and finally in **Ads -Fe1**, **Ads-Cr4**, **Ads-Mg2**. Therefore, the formation of M-O stable bonds is preferred in the order of Li, K, Na > Ca, Al > Fe, Cr, and Mg, consistent with the difference in adsorption energy values above.

4. CONCLUSIONS

Theoretical results indicate that the cation exchange into the lattice structure of kaolinite is unfavorable and endothermic. In contrast, the adsorption of metal cations on kaolinite surfaces is preferred on both H-slab and O-slab in forming M-O bonds. The Li^+ , Mg^{2+} , and Ca^{2+} cations are adsorbed alternately to the H-slab and O-slab, in which Li^+ and Mg^{2+} insert into the lattice structure of kaolinite. The Na^+ , K^+ , and Cr^{3+} cations interact favorably with O sites on the O-slab at the octahedral cage. In addition, the Al^{3+} and Fe^{3+} cations are located firmly at the tetrahedral cage on the H-slab. Metal cations adsorbed on kaolinite surfaces are regarded as chemical adsorptions and follow the sequence: $\text{Li}^+ > \text{K}^+ > \text{Na}^+ > \text{Ca}^{2+} > \text{Al}^{3+} > \text{Fe}^{3+} > \text{Cr}^{3+} > \text{Mg}^{2+}$. The formation of configurations leads to little changes in VB and CB and band gap energy. Noticeably, the exchange and adsorption of Fe^{3+} and Cr^{3+} onto kaolinite indicate a considerable difference in DOS and a substantial decrease in E -gap compared to other metal cations. Besides, the ELF analysis shows that the M-O contacts formed in configurations are chemical bonds.

REFERENCES

1. R. G. Harris, J. D. Wells, B. B. Johnson. Selective adsorption of dyes and other organic molecules to kaolinite and oxide surfaces, *Colloids Surfaces A Physicochem. Eng. Asp.*, **2001**, *180*, 131–140.
2. J. Chen, F. Fei Min, L. Liu, C. Liu, F. Lu. Experimental investigation and DFT calculation of different amine/ammonium salts adsorption on kaolinite, *Appl. Surf. Sci.*, **2017**, *419*, 241–251.
3. S. Zhang, J. J. Sheng, Z. Qiu. Water adsorption on kaolinite and illite after polyamine adsorption, *J. Pet. Sci. Eng.*, **2016**, *142*, 13–20.
4. E. R. Johnson and O. D. L. R. Alberto. Adsorption of organic molecules on kaolinite from the exchange-hole dipole moment dispersion model, *Journal of Chemical Theory and Computation*, **2012**, *8*, 5124–5131.
5. X. Wang, Y. Huang, Z. Pan, Y. Wang, C. Liu. Theoretical investigation of lead vapor adsorption on kaolinite surfaces with DFT calculations, *Journal of Hazardous Materials*, **2015**, *295*, 43–54.
6. D. J. Groenendijk and J. N. M. Wunnik. Surfactant Adsorption and Ion Exchange on Calcite Surfaces, *Energy Fuels*, **2021**, *35*, 8763–8772.
7. J. Hafner. Ab-initio simulations of materials using VASP: Density-functional theory and beyond, *Journal of Computational Chemistry*, **2008**, *29*(13), 2044–2078.
8. P. Perdew, K. Burke. Generalized gradient approximation made simple, *Phys. Rev. Lett.*, **1996**, *77*, 3865–3868.
9. C. E. White, J. L. Provis, T. Proffen, D. P. Riley, and J. S. J. Deventer. Density Functional Modeling of the Local Structure of Kaolinite Subjected to Thermal Dehydroxylation, *J. Phys. Chem. A*, **2010**, *114*, 4988–4996.
10. K. Koumpouras and J. A. Larsson. Distinguishing between chemical bonding and physical binding using electron localization function (ELF), *J. Phys.: Condens. Matter*, **2020**, *32*, 315502 (1-12).